Mechanical, Thermal, and Interfacial Properties of Green Composites with Ramie Fiber and Soy Resins

JUN TAE KIM AND ANIL N. NETRAVALI*

Department of Fiber Science and Apparel Design, Cornell University, 201 Martha Van Rensselaer Hall, Ithaca, New York 14853-4401

Fully biodegradable, green composites were fabricated with ramie fibers and modified soy flour (MSF) resin. Defatted soy flour (SF) was modified by a lab-scale filtration system to improve its mechanical, interfacial, and thermal properties through increasing the protein content. The protein content of SF was increased from 53.1 to 67.5% by filtering out soluble sugars using a microfiber-based filter. Tensile stress and Young's modulus of MSF resins were 35.5 and 1411.7 MPa, respectively, which were significantly higher than those (12.7 and 379.3 MPa) of SF resins. Interfacial shear strength of single ramie fibers with MSF resins ranged from 8.8 to 15.2 MPa, which were about 40−50% higher than those obtained with SF resins. Tensile stress and Young's modulus of ramie fiber-reinforced composites were 88.0 MPa and 2.94 GPa with SF resin and 103.8 MPa and 3.15 GPa with MSF resin.

INTRODUCTION

The use of plastics and fiber-reinforced composites has increased significantly in the past few decades. Most of these plastics such as polyolefins, polyvinyl chloride (PVC), polyesters, nylons, and epoxies and many fibers, however, are made using petroleum as feedstock. Unfortunately, these petroleum-based plastics have caused a significant part of the air, soil, and water pollution as a result of indiscriminate dumping combined with their nonbiodegradable nature and toxicity (*1−3*). Although recycling of the plastic waste is one of the solutions to avoid these environmental problems, in many cases, it is cost prohibitive to collect the waste. While a small part of the plastic waste is incinerated, most of it still ends up in the landfills. The U.S. Environmental Protection Agency (U.S. EPA) has reported that out of about 30.7 million tons of plastic waste of the municipal solid waste generated in the United States in 2007, only 6.8% of the plastic waste was recycled (*4*). Environmental consciousness among people, fast depletion of the petroleum reserves, and government regulations at many levels have spurred efforts to develop fully biodegradable, eco-friendly, and sustainable, so-called "green" materials to replace the nonbiodegradable plastics (*5−7*).

Natural cellulosic fibers such as flax, jute, ramie, hemp, sisal, and pineapple have attracted attention as reinforcements for composites due to many advantages such as annually renewable, sustainable, low cost, high specific modulus, lightweight, biodegradable, and biocompatible features (*8−11*). Many researchers have studied the development of advanced composites using natural fibers as reinforcements and epoxies or thermoplastics as resins to replace the metals in aerospace and automotive applications (*12−14*). Because the epoxies and thermoplastics are nonbiodegradable resins, these partially biodegradable or "semigreen" composites have the same disposal problems at the end of their life. They can neither return to an industrial metabolism nor return to a natural metabolism (*5*). Because the composite materials are fabricated by combining two dissimilar materials, it is hard to recycle and reuse them, particularly if thermoset resins are used. To avoid the disposal problems, both reinforcement and resin in composites could be made biodegradable. At the end of their lives, they can be easily composted. Only a few research papers in the recent past have been published on the development of the fully biodegradable, "green" composites using natural fibers and biodegradable resins such as polysaccharides and proteins (*15−17*).

Ramie is a bast fiber obtained from the perennial herbaceous plant, *Boehmeria nivea*, from the Urticaceae family. Ramie fibers are mainly grown in Korea, Japan, China, India, and other eastern Asian countries and are characterized by their high specific strength and modulus (*18*). The tensile stress, Young's modulus, and tensile strain of ramie fibers have been reported to be in the range of 400−938 MPa, 61−128 GPa, and 1.2−3.8%, respectively, which are dependent on the location and processing conditions (*10*). As a result, ramie fibers have been widely used as reinforcements in the green composites as well as in ropes (*19,20*). Soy bean protein is one of the most widely used biopolymers to fabricate green composites with natural fibers because they are annually renewable, inexpensive, biodegradable, and biocompatible and they have good strength (*21*). Soy protein contains many polar and reactive amino acids such as glutamic acid, aspartic acid, lysine, arginine, serine, threonine, and tyrosine that contain carboxyl (−COOH), amine (−NH$_2$), or hydroxyl (−OH) groups.

---

*To whom correspondence should be addressed. Tel: 607-255-1875. Fax: 607-255-1093. E-mail: ann2@cornell.edu.

These reactive groups could be used for inter- and intramolecular cross-linking, resulting in improved mechanical and thermal properties. There are three commercially available soy proteins based on their protein content: defatted soy flour (SF), soy protein concentrate (SPC), and soy protein isolate (SPI). While SF is the least purified soy product obtained by removing the oil from native soy beans, SPC and SPI are further purified products where soluble sugars have been removed to obtain a higher protein content. SF contains about 53% protein and 32% carbohydrates (primarily fructose, glucose, sucrose, raffinose, and stachyose), while SPC and SPI contain 72 and 90% protein, respectively (*22*). Because of the increased processing costs and lower yield as a result of carbohydrate removal, SPC and SPI are much more expensive as compared to SF. To consider the competitive economic price with the petroleum-based plastic materials, it is better to use the less expensive SF ($0.30/lb) than SPC (over $1.00/lb) and SPI (over $2.00/lb) (*23*). Although it is the most economic soy product, SF has shown poor mechanical properties as compared to SPC and SPI (*16*, *19*, *24*).

In the present study, SF was modified by removing the soluble sugars using a lab-scale filtration system to increase its protein content and thus the mechanical, interfacial, and thermal properties of the resin. These improvements can result in higher composite properties through better resin properties as well as better fiber/resin bonding. A durable and reusable microfiber-based fabric was used as the filtration media. The protein content of the modified soy flour (MSF) was obtained using a nitrogen analyzer and compared to the control SF. Attenuated total reflectance (ATR)−Fourier transform infrared (FTIR) spectra support that many of the soluble sugars could be successfully removed by a lab-scale filtration. Effects of protein content in soy resins (SF and MSF) on ramie fiber/soy resin interfacial properties and on the mechanical and thermal properties of ramie fiber-reinforced composites were investigated.

MATERIALS AND METHODS

Materials. SF was obtained from Archer Daniels Midland Co. (Decatur, IL). Unbleached ramie fibers in the form of Roving were supplied by Danforth International Trade Associates Inc. (Brielle, NJ). Sorbitol was purchased from Sigma Aldrich. Analytical grade sodium hydroxide (NaOH) and hydrochloric acid (HCl) were purchased from Fisher Scientific. Microfiber twill weave fabric (DF #CC611) was purchased from Denver Fabrics (St. Louis, MO).

Modification of Soy Flour (MSF). To increase the protein content, SF was modified by insolubilizing the protein and removing the soluble sugars using a lab-scale filtration system with microfiber-based fabric filter. SF was dissolved in water (10 times SF wt) by magnetic stirring at room temperature. When SF was completely dissolved, the SF solution was adjusted to pH 4.5 using HCl solution. At pH 4.5, the isoelectric point of soy protein, most of the protein becomes insoluble and precipitates while the sugars (fructose, glucose, sucrose, raffinose, and stachyose) are dissolved easily. The SF dispersion was then filtered using a reusable microfiber-based fabric filter. The retentate was rinsed twice with pure water to remove the remaining soluble sugars after which it was dried and ground into the powder form using a mortar and pestle to characterize its protein content and FTIR spectrum. To prepare the MSF resin, the wet MSF after filtration was directly used without drying it. After the sugars were removed, 60% of the original SF material was recovered. At the original SF cost of $0.30/lb, the MSF will cost about $0.50/lb. Even when a $0.05/lb is added as a processing cost, the MSF will cost $0.55/lb, significantly lower than over $1.00/lb for the SPC.

Analysis of Protein Content in MSF. Total nitrogen contents of both SF and MSF were measured using a nitrogen analyzer, LECO FP-528 (LECO Corp., St. Joseph, MI) using the Dumas type combustion method (*25*). The average of two replicates was used for the nitrogen content of MSF, and its protein content was calculated by multiplying a Kjeldahl factor of 6.25 (*26*).

ATR-FTIR Analysis. The composition changes in MSF were investigated using the ATR-FTIR spectrometer, model Nicolet Magna 560, with a Split Pea accessory. All spectra were obtained by averaging of 128 scans at a resolution of 4 cm^{-1} in the range of 4000 to 800 cm^{-1} wavelength.

Preparation of Soy Resin Sheets. Soy resins were prepared by slowly dissolving the soy proteins (SF and MSF) in deionized (DI) water with a ratio of 1:13 by weight. When soy proteins were completely dissolved, sorbitol was added as a plasticizer to overcome the brittleness of the soy resins. The amount of sorbitol was varied to assess its effect on the mechanical properties of the resins. After the pH of the soy resin solutions was adjusted to 10 using 1 M NaOH solution, they were precured at 75 °C in a water bath for 30 min. The precured soy resins were cast on the Teflon-coated glass plates and dried at 35 °C in an air-circulated drying oven for 16 h. Dried soy resin sheets were cured using a Carver Hydraulic hot press (model 3891-4PROAOO) at 120 °C for 25 min under a pressure of 7 MPa. The cured sheets were conditioned at 21 °C and 65% relative humidity (RH) for 72 h before their mechanical properties were characterized.

Fabrication of Ramie Fiber-Reinforced Green Composites. Fully biodegradable, green composites were fabricated using SF and MSF resins and ramie fibers. To fabricate composite sheets with 100 mm × 180 mm dimensions, 10 g of ramie fibers with 100 mm long was prepared, and small amounts of the ramie fibers were soaked in the precured soy resins and then squeezed by hand to remove the excess resins. This soaking/squeezing sequence was repeated several times to obtain complete impregnation of the fibers with the resins. The wet fiber bundles were hand-laid on the Teflon-coated glass plates by aligning them layer by layer and then drying them at 45 °C. Dried composite sheets were cured by hot pressing at 120 °C for 50 min under 7 MPa of pressure. The cured composite sheets were conditioned at 21 °C and 65% RH for 5 days before their tensile properties were characterized.

Tensile Properties of Resin Sheets. The cured soy resin sheets were cut into rectangular specimens of 100 mm × 10 mm to test their tensile properties. The tensile properties of soy resin sheets were characterized using Instron, model 5566 (Instron Co., Canton, MA), according to ASTM D882-02. A gauge length of 50 mm and a strain rate of 1 min^{-1} (crosshead speed of 50 mm/min) were used for all specimens. At least 10 specimens were tested to obtain the average values.

Ramie Fiber/Soy Resins Interfacial Shear Strength (IFSS). The IFSS of the ramie fiber and soy resins was evaluated using the microbond technique (*19*, *20*). To prepare the microbond test specimen, a single ramie fiber was mounted on a paper tab and glued at both ends using cyanoacrylate glue. Using the precured soy resins containing 0 and 20% (w/w soy protein) sorbitol, a small microdrop (microbead) was placed on the ramie fiber with the help of a 200 μm diameter sisal fiber. The fibers with microbeads were kept at room temperature before heating them at 120 °C in an oven for 60 min to cure the resin. This curing process has been shown to cross-link soy proteins (*20*). All specimens for the microbond tests were equilibrated at 21 °C and 65% RH for 24 h prior to testing. A schematic of the microbond test is shown in **Figure 1**. The fiber diameter, *D*, and embedded length, *L*, were measured prior to the microbond test using a calibrated optical microscope, model Nicolet Continuμm (Spectra-Tech Inc., United States). The microbond test was performed using Instron with a special microvise. The microvise plates were placed just above the microbead and brought closer until they barely touched the fiber surface as shown in **Figure 1**. The fiber was then pulled out from the microbead at a crosshead speed of 0.2 mm/min until the microbead debonded. The interfacial shear strength, τ, was calculated using the following equation:

$$\text{interfacial shear strength } (\tau) = \frac{F}{\pi \times D \times L} \tag{1}$$

where *F* is the force required to debond the microbead. It was assumed that the shear strength was uniform along the entire fiber/microbead interface. At least 20 successful tests were conducted to obtain the average IFSS values.

Tensile Properties of Composites. Tensile properties of unidirectional ramie fiber-reinforced green composites were characterized in parallel (longitudinal) and perpendicular (transverse) directions to the fiber axis. Tensile tests of the composites were performed according to ASTM D3039-00. The cured composite sheets were cut into rectangular
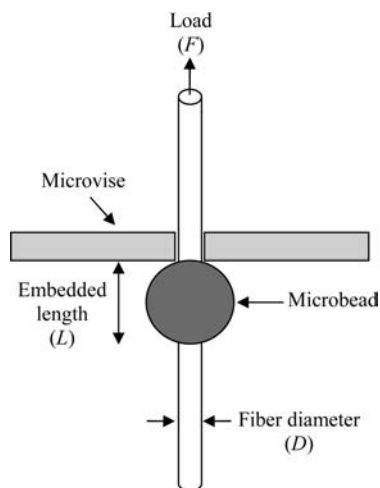
Figure 1. Schematic of the microbond test.

Table 1. Nitrogen and Protein Contents of the Control SF and MSF

soy proteins	nitrogen content (%)	protein content (%)
SF	8.5	53.1
MSF	10.8	67.5

strips (specimens) of 60 mm × 10 mm. A gauge length of 30 mm was maintained, and the strain rate was set at 0.05 min^{-1}. To prevent the specimen slippage from the grip during tensile testing, both ends of composite specimens were mounted on a paper tab using cyanoacrylate glue. At least seven specimens were tested to obtain the average values.

Characterization of Surface Properties. The fractured surfaces of the composites and the surface/cross-sectional images of ramie fibers were characterized using a scanning electron microscope (SEM; Leica model 440X, Cambridge, United Kingdom). The specimens were loaded on the SEM mount with double-sided electrically conductive adhesive carbon tape (SPI Supplies, West Chester, PA). The specimen mounts were coated with gold/palladium (Au/Pd) for 30 s with a 45 mA current in sputter coater. The coated specimens were observed on the SEM using an accelerating voltage of 5 kV.

Thermogravimetric Analysis (TGA). Thermal stability and decomposition of the components in the composites were investigated using TGA, model 2050 (TA Instruments, New Castle, DE). All specimens were scanned from 25 to 500 °C at a ramp rate of 20 °C/min in nitrogen environment. About 20 mg of specimen was used for each scan. TA Instruments software, Universal Analysis (version 2.5), was used to transform the TG curve to the derivative thermogravimetric (DTG) curve.

RESULTS AND DISCUSSION

Nitrogen/Protein Content of MSF. As mentioned earlier, protein-enriched MSF was obtained by removing the soluble sugars (fructose, glucose, sucrose, raffinose, and stachyose) using a lab-scale filtration system with a reusable microfabric filter. The nitrogen contents of both SF and MSF were obtained by a combustion analyzer, and its protein content was calculated by multiplying the commonly used Kjeldahl factor of 6.25 to the obtained nitrogen content (*26*). **Table 1** presents the nitrogen and protein contents in SF and MSF. The lab-scale filtration used in this study increased the protein content from 53.1% in SF to 67.5% in MSF, a significant increase of over 14%. Because the protein content of MSF was much higher, composite mechanical properties and fiber/resin interfacial shear strength of MSF could be expected to be higher than those of the control SF.

ATR-FTIR Spectra of MSF. The composition change of MSF was characterized using ATR-FTIR spectroscopy. **Figure 2** shows the FTIR spectra of the control SF and MSF powders. A typical soy protein spectrum shows three major peaks at 1638, 1537, and
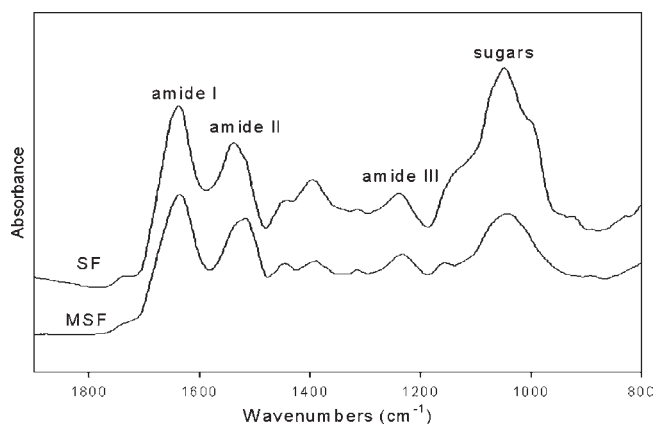

Figure 2. ATR-FTIR spectra of SF and MSF.

1238 cm^{-1}, which are assigned to C=O stretching (amide I band), N−H deformation (amide II band), and C−N stretching and N−H vibration (amide III band), respectively (*27, 28*). The SF spectrum shows another major peak at 1049 cm^{-1}, which is assigned to C−O stretching, indicating sugar molecules (*29*). This peak was significantly decreased in MSF as shown in **Figure 2**, indicating that a significant amount of the sugars was filtered out. This also confirms the higher protein amount in the MSF.

Characterization of Ramie Fiber. Tensile properties and moisture contents of ramie fibers are presented in **Table 2**. The high CV% for both tensile stress and modulus values indicates a large variation in tensile properties of ramie fiber. This is attributed to the inherent irregularity present in most natural fibers (*30*). Tensile stress, tensile strain, and Young's modulus of single ramie fibers were 333.48 MPa, 1.63%, and 24.71 GPa, respectively. The moisture content of ramie fibers was 5.85%. These tensile properties are lower than those reported by other researchers (*10, 19*), mainly due to the long aging and storage in the lab. The surface and cross-sectional shapes of ramie fibers were investigated using SEM. **Figure 3a** shows a SEM microphotograph of ramie fiber's surface, which is very clean, smooth, and relatively uniform. The average diameter of the ramie fiber was around 25−30 μm. **Figure 3b** shows the SEM photomicrograph of the cross-sectional view of ramie fibers. As shown in **Figure 3b**, the cross-section of ramie fibers is ellipsoidal in shape and has a large lumen surrounded by several wall layers. This hollow and layered structure of ramie fiber can provide good soundproofing and thermal insulation properties (*31*).

Tensile Properties of Soy Resins. Soy resin sheets were prepared at pH 10 with 0, 10, 20, and 30% (w/w soy protein) sorbitol as a plasticizer. At the alkaline condition (pH 10), the soy protein molecules can be denatured and open (unfolded) form, making it easy to process (*32*). **Figure 4** shows the effect of sorbitol content on the tensile properties and moisture content of SF and MSF resins. The strength and stiffness of MSF resin showed significant improvement as compared to those of SF resin. Tensile stress and Young's modulus of soy resins without plasticizer were 12.70 and 379.30 MPa for SF resin and 35.48 and 1411.78 MPa for MSF resin, respectively. Tensile stress and Young's modulus of SF resin could be improved about three times by the modification using a lab-scale filtration system. The least processed SF contains only 53.1% protein, while it still contains 32% carbohydrates. While carbohydrates in soy proteins include a small amount of dietary fibers such as cellulose, the major content is in the form of small sugars such as fructose (monomer), glucose (monomer), sucrose (dimer), raffinose (trimer), and stachyose (tetramer) (*33*). Although they are relatively larger molecules than the plasticizer (sorbitol) used, these sugars are still many times

smaller than the soy protein molecules. As a result, they also tend to plasticize the soy resin. These sugar molecules also could increase the moisture absorption by the soy resin sheets resulting in additional plasticizing. Because of the high content of sugars and their plasticizing effect, SF resin has poor strength and stiffness (modulus) (*34*). Improvement of the strength and stiffness of MSF resin, as compared to SF, is attributed to the higher

Table 2. Tensile Properties and Moisture Content of Ramie Fibers

tensile stress (MPa)	tensile strain (%)	Young's modulus (GPa)	moisture content (%)
333.48 (23.85)[a]	1.63 (15.70)	24.71 (26.92)	5.85

[a] Numbers in parentheses indicate the percent coefficient of variation.

protein content and reduced sugar content. The effect of plasticizer on tensile properties was investigated by varying the sorbitol content from 0 to 30% (w/w soy protein). As expected, tensile stress and Young's modulus significantly decreased with increased sorbitol content, while tensile strain increased in both SF and MSF resins as a result of plasticization. However, tensile strain of SF and MSF resins was not significantly different ($P > 0.05$) with over 20% sorbitol content. This is because the plasticization effect of sorbitol is much higher than small sugars in SF resin. The moisture content also increased with sorbitol content due to its more hydrophilic nature as shown in **Figure 4d**. To evaluate the plasticizing effect of the small sugars in soy protein, the data in **Figure 4** were modified to present the tensile properties of the soy resins as a function of the total plasicizer
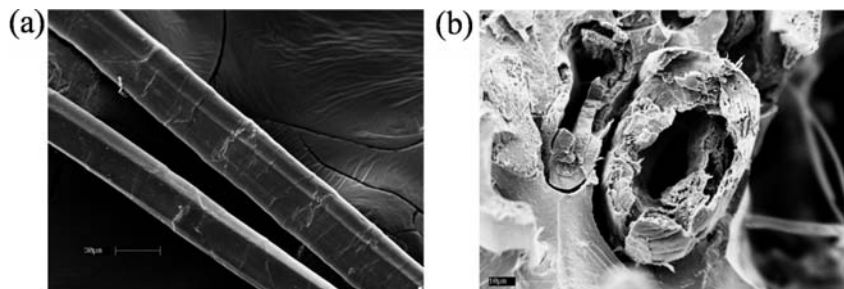

Figure 3. SEM photomicrographs of (**a**) surface and (**b**) cross-section images of ramie fibers.
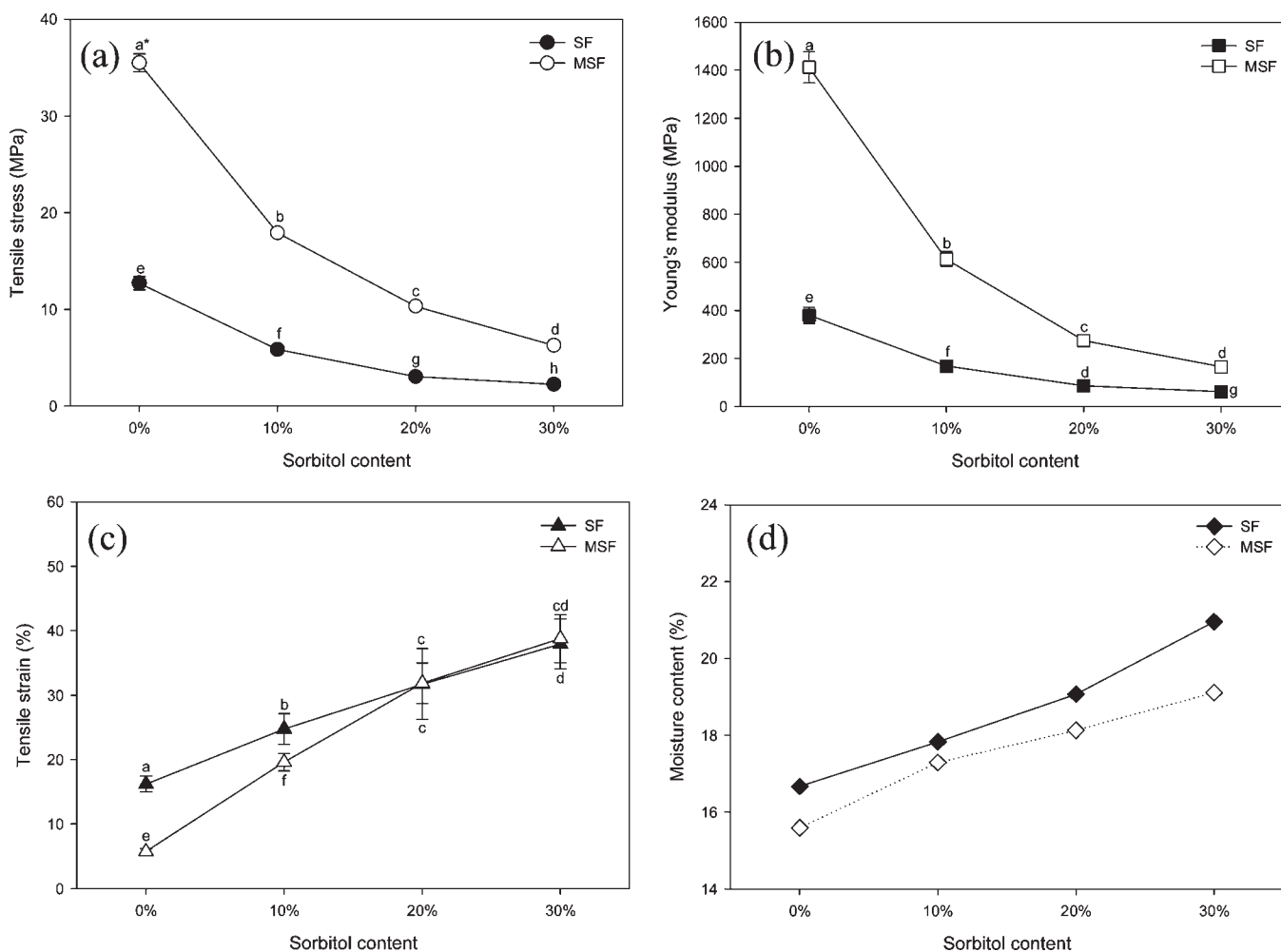

Figure 4. Effect of sorbitol content on the tensile properties and moisture content of SF and MSF resins. *Alphabets indicate a significant difference at $P < 0.05$ by ANOVA test.
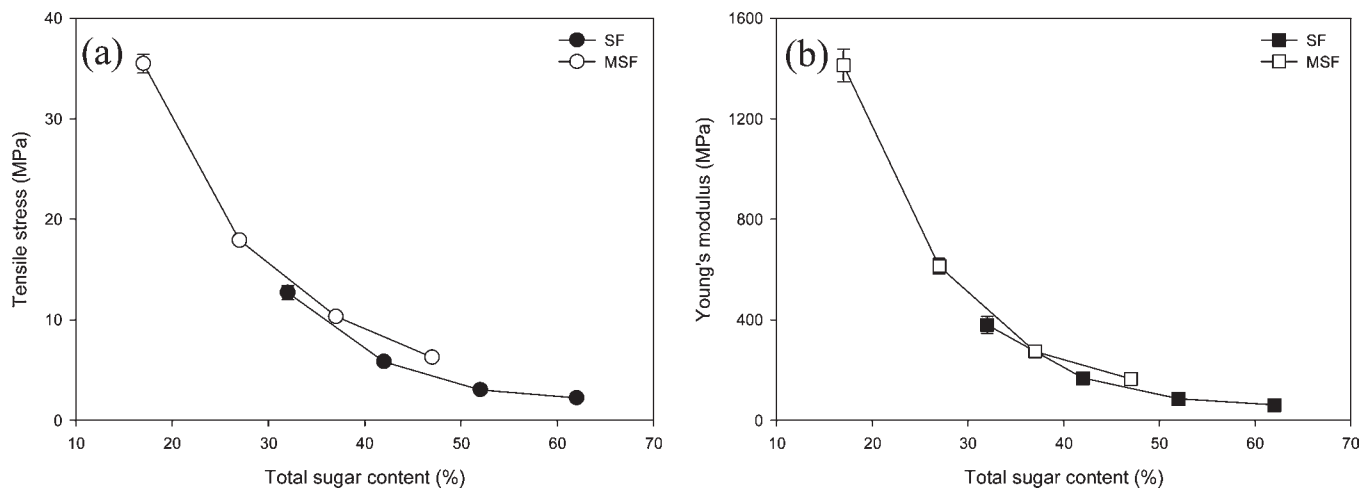
5404 *J. Agric. Food Chem.,* Vol. 58, No. 9, 2010

Kim and Netravali

Figure 5. Tensile stress and Young's modulus of soy resins as a function of sugars + sorbitol.
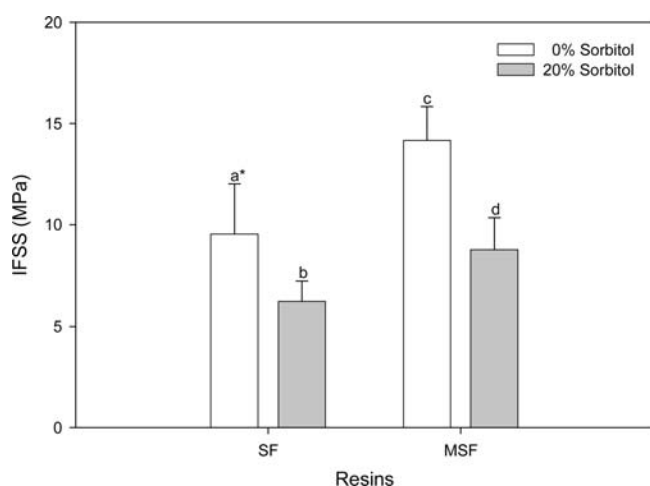

Figure 6. IFSS of ramie fiber with SF and MSF resins with 0 and 20% sorbitol. *Alphabets indicate a significant difference at $P < 0.05$ by ANOVA test.

content (sugars + sorbitol). **Figure 5** shows the tensile stress and Young's modulus of SF and MSF resins as a function of the total plasticizer content. Both tensile stress and Young's modulus of soy resins decreased with total sugar content, as can be expected. Because the two plots overlap well, it may be concluded that most small sugars in soy protein could act as a plasticizer and that the effect of the sugars is similar to that of sorbitol.

Ramie Fiber/Soy Resin IFSS. Figure 6 shows the comparison of IFSS values between single ramie fibers and soy resins with 0 and 20% sorbitol obtained using microbond test. Although the strength and stiffness (modulus) of fiber-reinforced composites mainly depend on the fiber strength, polymeric resin keeps the fibers in place, and importantly, it is responsible for transferring the load between the neighboring fibers. The load transfer efficiency, which depends on the fiber/resin bonding, is considered to be another important factor in determining the composite strength, modulus, and toughness. Higher fiber/resin IFSS results in better composite properties (*35*). On the other hand, lower IFSS increases the toughness of the composites. The IFSS of ramie fiber also significantly ($P < 0.05$) increased by the modification of SF from 9.53 to 14.17 MPa without plasticizer and from 6.24 to 8.76 MPa with 20% sorbitol. This result clearly indicates that a higher protein content of the soy resin results in higher IFSS with ramie fibers. Because the sugar chemistry is similar to cellulosic fibers, strong fiber/carbohydrate hydrogen

bonding can be expected. However, lower molecular weight sugars in SF plasticize the soy resin, which, then, can be easily sheared and debonded from the fiber surface resulting in lower IFSS value. As shown in the earlier study (*36*), the IFSS of ramie fiber/soy resins significantly decreased with plasticizer concentration. The plasticization effect on the IFSS was more significant with MSF resin that had a higher protein content. Even though some carbohydrates in soy protein can reduce the interfacial adhesion strength with natural fibers, IFSS of ramie fiber and soy protein resins was still higher than the IFSS values obtained for natural fibers with many thermoplastic polymers. For example, Luo and Netravali (*37*) reported that IFSS of henequen fibers and poly(hydroxybutyrate-co-valerate) (PHBV) resin using microbond technique was 5.24 MPa. Li et al. (*38*) reported that sisal fiber/high density polyethylene (HDPE) resin IFSS, measured using the single fiber pull-out technique, ranged between 1.5 and 3.0 MPa. These low IFSS values were primarily because of the chemical mismatch between the cellulosic fibers with polar surface and PHBV and/or the HDPE resins with nonpolar character resulting in no hydrogen bonding. In addition, the high viscosity of these polymers prevented their wetting, spreading, and filling any valleys in the fiber surface preventing any mechanical bonding. The ramie fiber/soy resin interfacial adhesion in real composites would be expected to be significantly better than that obtained by the microbond test because the composites are fabricated by hot pressing during which the resin is forced to flow inside the fiber surface valleys and thus increase the mechanical interlocking between fibers and resins. This should also result in better mechanical properties of the composites than can be predicted from the IFSS values.

Tensile Properties of Ramie Fiber/SF and MSF Composites. Unidirectional green composites, composite I and composite II, were fabricated with the precured SF resin and MSF resin, respectively. To prevent the composites failure by the brittleness of soy resins, 20% (w/w soy protein) sorbitol was added to the soy resins for the composites. The fiber content in the composites was kept close to 50% (w/w). Tensile properties of the ramie fiber-reinforced composites with SF and MSF resins in both longitudinal and transverse directions are presented in **Table 3**. The tensile stress and Young's modulus of the composites in longitudinal direction were 88.0 MPa and 2.94 GPa with SF resin and 103.8 MPa and 3.15 GPa with MSF resin, respectively. It was expected that the MSF with a higher protein content would result in higher tensile properties. While the tensile stress and modulus increased by about 18 and 7%, respectively, the tensile strain was

Table 3. Tensile Properties of Ramie Fiber-Reinforced Composites with SF and MSF Resins Containing 20% Sorbitol

resins	test direction	tensile stress (MPa)	tensile strain (%)	Young's modulus (GPa)	moisture content (%)
composite I (SF resin)	longitudinal	87.99 (4.67)[a]	4.26 (7.54)	2.94 (8.66)	12.98
	transverse	2.77 (12.65)	2.43 (15.71)	0.27 (11.48)	
composite II (MSF resin)	longitudinal	103.81 (11.19)	4.24 (11.62)	3.15 (15.44)	10.82
	transverse	6.04 (11.83)	1.38 (12.05)	0.60 (5.37)	

[a] Numbers in parentheses indicate the percent coefficient of variation.
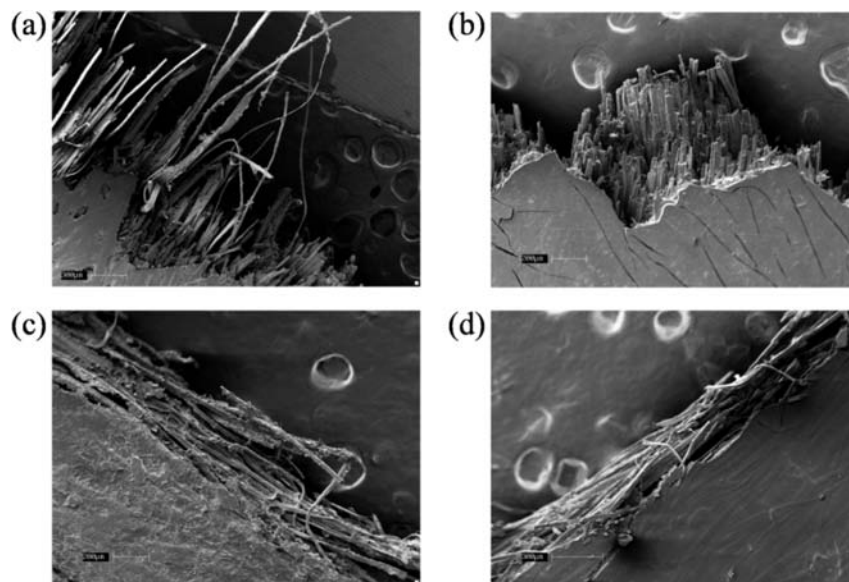
Figure 7. SEM photomicrographs of the fracture surface of composite I and composite II.

around 4.25% for both soy resins. This is not surprising since the composite fracture strain is controlled by the fiber fracture strain. Tensile properties of the composites in transverse direction clearly showed a good correlation with the resin properties. The tensile stress and Young's modulus of the composites in transverse direction also improved from 2.77 MPa and 0.27 GPa, respectively, for SF resin to 6.04 MPa and 0.60 GPa for MSF resin. Because the unidirectional composite properties in transverse direction are mainly dependent on the resin properties and/or fiber/resin interfacial properties, these results also support that a higher protein content in soy resins could increase both resin properties and fiber/resin IFSS, resulting in higher transverse properties of the composites. The strength of these composites showed superior properties as compared to the natural fiber-reinforced−thermoplastic (HDPE) composites reported by Facca et al. (*39*). The poor strength in natural fiber−thermoplastic composites is mainly due to the poor interfacial adhesion between fibers and thermoplastic resin. Liu et al. (*40*) developed soy flour-based biocomposites with pineapple leaf fiber using an injection molding. Maximum tensile strength and modulus of the biocomposites were about 33 MPa and 4 GPa, respectively, with 30% volume fraction of pineapple leaf fiber. These values are much lower than the properties obtained in this study mainly because of the lower volume fraction.

It is clear from these data that the variation in tensile properties of the composites is much lower than that of the fibers. This is generally true for all composites since the variation of the fibers is averaged out in composites that contain many fibers in the cross-section. In addition, the fiber cross-sections are not uniform, particularly for the natural fibers, whereas the composites have uniform thickness as they are hot pressed between two plates.

Characterization of Composite Fracture Surfaces. Figure 7 shows SEM photomicrographs of the surfaces fractured in

longitudinal and transverse directions of ramie fiber-reinforced composites with SF (**a** and **c**) and MSF (**b** and **d**) resins. As can be clearly seen in **Figure 7a**, SF resin composites in longitudinal direction show longer fibers being pulled out from the resins and also less resin sticking to the surfaces of the fibers that were pulled out. In the case of MSF resin composites, the pulled out fiber length was smaller, and higher amounts of resin were sticking to the pulled out fibers. Similar results were observed in the transverse direction as well. Also, some fibers in SF resin-based composites were separated, whereas the fibers in MSF resin-based composites were found to be sticking together after the fracture test, as can be seen in **Figure 7a,b**. The amount of resin sticking to the pulled out fiber surfaces shows good correlation with the protein content in the resin and the resulting fiber/resin IFSS. These SEM results support that the ramie fiber/soy resin IFSS increased with a higher protein content. In the previous study of soy protein IFSS, soy protein resins were seen to rarely remain on the fiber surfaces after microbond test (*36*). However, a lot of soy resin was observed on the fractured fiber surface of the composites. As mentioned earlier, this was because of the mechanical interlocking between the fibers and the resins resulting from the hot pressing of composites during fabrication. The higher extent of mechanical interlocking of fibers and soy protein resins should increase not only the interfacial adhesion strength but also the tensile strength of the composites.

Thermal Degradation of Composites. The thermal stability of the composite I (SF resin) and the composite II (MSF resin) was characterized using TGA analysis. **Figure 8a,b** shows the TG and DTG curves of ramie fiber-reinforced composites with SF and MSF resins. For a better view of the weight loss, TG curves were transformed into their first derivative (Δ weight loss/Δ temperature) curves (DTG) using the TA software, Universal Analysis (version 2.5). Composite I revealed three distinct weight
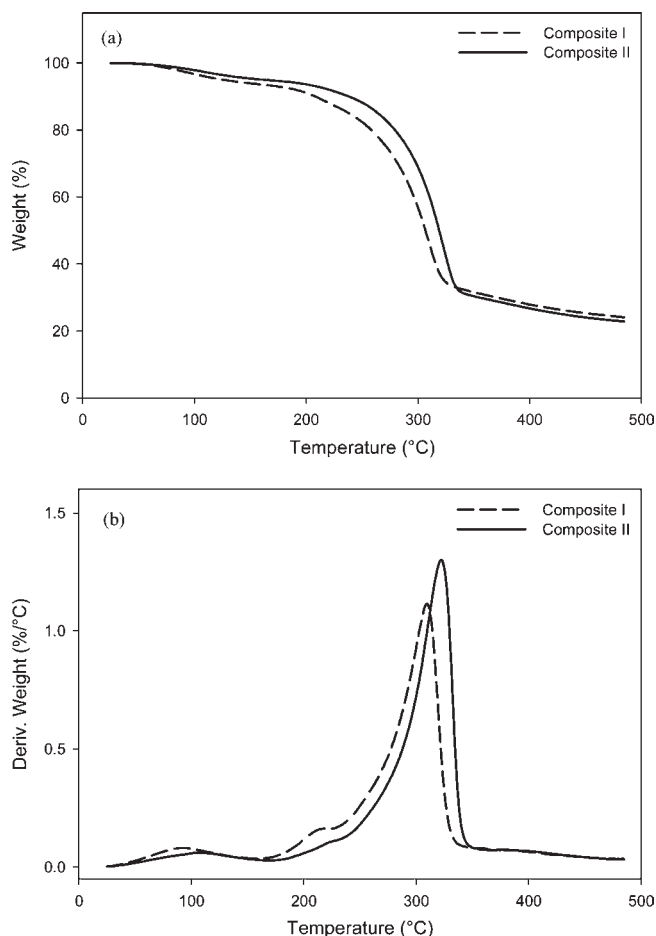
Figure 8. TG (**a**) and DTG (**b**) of composite I and composite II.

loss stages as seen in **Figure 8b**. The first stage observed between 70 and 120 °C is primarily associated with the loss water. The second and third stages are associated with the thermal degradation of the components in the composites. The second stage observed between 180 and 215 °C is mainly associated with the low molecular weight sugars such as glucose, fructose, sucrose, raffinose, stachyose, and sorbitol used as a plasticizer (*41*, *42*). The third stage observed between 250 and 340 °C is associated with the decomposition of soy protein and fiber components such as hemicelluloses and cellulose. The beginning of the third stage could be the degradation of soy protein, while the end part would be the degradation of fiber components. Composite II shows thermal behavior similar to that of composite I, but the TG and DTG curves of the composite II revealed significant thermal improvement. All peaks of composite II were shifted to higher temperatures as shown in **Figure 8b**. The first stage is associated with the loss of water. The second stage of composite II was observed between 190 and 230 °C, but its intensity was much lower than that of composite I. This is because of the significantly lower sugar content of the MSF resin. This result also supports our observation that most soluble sugars were successfully removed in MSF resin, resulting in improvement of thermal stability in the resin and the composites as well. The temperature range of the third stage also moved to a higher value. The maximum decomposition temperature (T_m) of composite II was 322 °C, which was 13 °C higher than the T_m of composite I. In addition, the area under the third stage is significantly higher that obtained for composite I. This is mainly due to the increased protein content in MSF.

LITERATURE CITED

(1) Bean, M. L. Legal strategies for reducing persistent plastics in the marine environment. *Mar. Pollut. Bull.* **1987**, *18*, 357–360.

(2) Mulder, K.; Knot, M. PVC plastic: A history of systems development and entrenchment. *Technol. Soc.* **2001**, *23*, 265–286.

(3) Derraik, J. G. B. The pollution of the marine environment by plastic debris: a review. *Mar. Pollut. Bull.* **2002**, *44*, 842–852.

(4) EPA. *Municipal Solid Waste Generation, Recycling and Disposal in the United States: 2007 Facts and Figures*; EPA: Washington, DC, 2008.

(5) Netravali, A. N.; Chabba, S. Composites get greener. *Mater. Today* **2003**, *6*, 22–29.

(6) Goda, K.; Cao, Y. Research and development of fully green composites reinforced with natural fibers. *J. Solid Mech. Mater. Eng.* **2007**, *1*, 1073–1084.

(7) Mohanty, A. K.; Misra, M.; Drzal, L. T. Sustainable bio-composites from renewable resources: Opportunities and challenges in the green materials world. *J. Polym. Environ.* **2002**, *10*, 19–26.

(8) Dahlke, B.; Larbig, H.; Scherzer, H. D.; Poltrock, R. Natural fiber reinforced foams based on renewable resources for automotive interior applications. *J. Cell. Plast.* **1998**, *34*, 361–379.

(9) Bledzki, A. K.; Gassan, J. Composites reinforced with cellulose based fibres. *Prog. Polym. Sci.* **1999**, *24*, 221–274.

(10) Mohanty, A. K.; Misra, M.; Hinrichsen, G. Biofibres, biodegradable polymers and biocomposites: An overview. *Macromol. Mater. Eng.* **2000**, *276/277*, 1–24.

(11) Wambua, P.; Ivens, J.; Verpoest, I. Natural fibres: Can they replace glass in fibre reinforced plastics? *Compos. Sci. Technol.* **2003**, *63*, 1259–1264.

(12) Roe, P. J.; Ansell, M. P. Jute-reinforced polyester composites. *J. Mater. Sci.* **1985**, *20*, 4015–4020.

(13) Hughes, M.; Hill, C. A. S.; Hague, J. R. B. The fracture toughness of bast fibre reinforced polyester composites. Part 1. Evaluation and analysis. *J. Mater. Sci.* **2002**, *37*, 4669–4676.

(14) Acha, B. A.; Reboredo, M. M.; Marcovich, N. R. Creep and dynamic mechanical behavior of PP-jute composites: Effect of the interfacial adhesion. *Composites, Part A* **2008**, *38*, 1507–1516.

(15) Luo, S.; Netravali, A. N. Mechanical and thermal properties of environment-friendly "green" composites made from pineapple leaf fibers and poly(hydroxybutyrate-co-valerate) resin. *Polym. Compos.* **1999**, *20*, 367–378.

(16) Chabba, S.; Matthews, G. F.; Netravali, A. N. 'Green' composites using cross-linked soy flour and flax yarns. *Green Chem.* **2005**, *7*, 576–581.

(17) Takagi, H.; Asano, A. Characterization of "green" composites reinforced by cellulose nanofibers. *Key Eng. Mater.* **2007**, *334/335*, 389–392.

(18) Liu, F.; Liang, X.; Zhang, Z.; Huang, Y.; Zhang, S. Effect of growth regulators on yield and fiber quality in ramie (*Boemheriz nivea* (L.) Gaud.), China grass. *Field Crops Res.* **2001**, *69*, 41–46.

(19) Lodha, P.; Netravali, A. N. Characterization of interfacial and mechanical properties of "green" composites with soy protein isolate and ramie fiber. *J. Mater. Sci.* **2002**, *37*, 3657–3665.

(20) Nam., S.; Netravali, A. N. Characterization of ramie fiber/soy protein concentrate (SPC) resin interface. *J. Adhes. Sci. Technol.* **2004**, *18*, 1063–1076.

(21) Swain, S. N.; Biswal, S. M.; Nanda, P. K.; Nayak, P. L. Biodegradable soy-based plastics: Opportunities and challenges. *J. Polym. Environ.* **2004**, *12*, 35–42.

(22) http://www.admworld.com/naen/productdb/default.aspx.

(23) Weingartner, K.; Owen, B. *Soy Protein Applications in Nutrition & Food Technology*; World Initiative for Soy in Human Health (WISHH) Workshops: Washington, DC, 2009.

(24) Nam, S.; Netravali, A. N. Green composites. II. Environment-friendly, biodegradable composites using ramie fibers and soy protein concentrate (SPC) resin. *Fibers Polym.* **2006**, *7*, 380–388.

(25) AOAC. Protein (crude) in animal feed combustion method (Dumas method). *AOAC Official Methods of Analysis 1989*, 17th ed.; Method 990.03; AOAC: Washington, DC, 2002.

(26) Berner, D. L.; Brown, J. Protein nitrogen combustion method collaborative study I. Comparison with smalley total Kjeldahl nitrogen and combustion results. *J. Am. Oil Chem. Soc.* **1994**, *71*, 1291–1293.

(27) Subirade, M.; Kelly, I.; Gueguen, J.; Pezolet, M. Molecular basis of film formation from a soybean protein: comparison between the conformation of glycinin in aqueous solution and in films. *Int. J. Biol. Macromol.* **1998**, *23*, 241–249.

(28) Soares, R. M. D.; Scremin, F. F.; Soldi, V. Thermal stability of biodegradable films based on soy protein and corn starch. *Macromol. Symp.* **2005**, *229*, 258–265.

(29) Kačuráková, M.; Mathlouthi, M. FTIR and laser-Raman spectra of oligosacchairdes in water: Characterization of the glycosidic bond. *Carbohydr. Res.* **1996**, *284*, 145–157.

(30) Bismarck, A.; Mishra, S.; Lampke, T. Plant Fibers as Reinforcement for Green Composites. In *Natural Fibers, Biopolymers, and Biocomposites*; Mohanty, A. M., Misra, M., Drzal, L. T., Eds.; CRC Press: Boca Raton, FL, 2005; pp 37−108.

(31) Beckmann, F. Sound and heat insulation material. U.S. Patent 6914020 B1, 2005.

(32) Gennadios, A.; Brandenburg, A. H.; Weller, C. L.; Testin, R. F. Effect of pH on properties of wheat gluten and soy protein isolate films. *J. Agric. Food Chem.* **1993**, *41*, 1835–1839.

(33) Sarkar, P. K.; Jones, L. J.; Craven, G. S.; Somerset, S. M. Oligosaccharide profiles of soybeans during kinema production. *Lett. Appl. Microbiol.* **1997**, *24*, 337–339.

(34) Rathi, P. Soy protein based nano-phase resins for green composites. M.S. Thesis, Cornell University, Ithaca, NY, **2007**.

(35) Xiaoyu, J.; Xiangan, K. Micro-mechanical characteristics of fiber/matrix interfaces in composite materials. *Compos. Sci. Technol.* **1999**, *24*, 635–642.

(36) Kim, J. T.; Netravali, A. N. Effect of protein content in soy protein resins on their interfacial shear strength with ramie fibers. *J. Adhes. Sci. Technol.* **2010**, *24*, 203–215.

(37) Luo, S.; Netravali, A. N. Characterization of henequen fibers and the henequen fiber/poly(hydroxybutyrate-co-hydroxyvalerate) interface. *J. Adhes. Sci. Technol.* **2001**, *15*, 423–437.

(38) Li, Y.; Hu, C.; Yu, Y. Interfacial studies of sisal fiber reinforced high density polyethylene (HDPE) composites. *Composites, Part A* **2008**, *39*, 570–578.

(39) Facca, A. G.; Kortschot, M. T.; Yan, N. Predicting the tensile strength of natural fibre reinforced thermoplastics. *Compos. Sci. Technol.* **2007**, *67*, 2454–2466.

(40) Liu, W.; Misra, M.; Askeland, P.; Drzal, L. T.; Mohanty, A. K. 'Green' composites from soy based plastic and pineapple leaf fiber: Fabrication and properties evaluation. *Polymer* **2005**, *46*, 2710–2721.

(41) Yan, W.; Suppes, G. J. Vapor pressures and evaporation studies of sugars and sugar alcohols. *J. Chem. Eng. Data* **2008**, *53*, 2033–2040.

(42) Schwarz, E. M.; Grundstein, V. V.; Ievins, A. F. Thermal investigation of polyols. I. Hexitols and pentitols. *J. Therm. Anal.* **1972**, *4*, 331–337.